Acta Crystallographica Section D
Biological Crystallography
ISSN 0907-4449

Distal histidine conformational flexibility in dehaloperoxidase from *Amphitrite ornata*

Zuxu Chen,[a] Vesna de Serrano,[a] Laurie Betts[b] and Stefan Franzen[a]*

[a]Department of Chemistry, North Carolina State University, Raleigh, NC 27695, USA, and [b]Biomolecular X-ray Structure Facility, University of North Carolina School of Medicine, Chapel Hill, NC 27599, USA

Correspondence e-mail: stefan_franzen@ncsu.edu

Received 5 August 2008
Accepted 6 November 2008

PDB Reference: deoxy dehaloperoxidase, 3dr9, r3dr9sf.

The enzyme dehaloperoxidase (DHP) from the terebellid polychaete *Amphitrite ornata* is a heme protein which has a globin fold but can function as both a hemoglobin and a peroxidase. As a peroxidase, DHP is capable of converting 2,4,6-trihalophenols to the corresponding 2,6-dihaloquinones in the presence of hydrogen peroxide. As a hemoglobin, DHP cycles between the oxy and deoxy states as it reversibly binds oxygen for storage. Here, it is reported that the distal histidine, His55, exhibits conformational flexibility in the deoxy form and is consequently observed in two solvent-exposed conformations more than 9.5 Å away from the heme. These conformations are analogous to the open conformation of sperm whale myoglobin. The heme iron in deoxy ferrous DHP is five-coordinate and has an out-of-plane displacement of 0.25 Å from the heme plane. The observation of five-coordinate heme iron with His55 in a remote solvent-exposed conformation is consistent with the hypothesis that His55 interacts with heme iron ligands through hydrogen bonding in the closed conformation. Since His55 is also displaced by the binding of 4-iodophenol in an internal pocket, these results provide new insight into the correlation between heme iron ligation, molecular binding in the distal pocket and the conformation of the distal histidine in DHP.

1. Introduction

The enzyme dehaloperoxidase (DHP), which was first isolated from the terebellid polychaete *Amphitrite ornata*, is a heme-containing peroxidase which functions as both a globin and a peroxidase. While all hemoglobins possess some peroxidase activity, the activity of DHP is significantly greater than that of any known native hemoglobin. As is well known, oxygen binding is a reversible process that is common to all ferrous hemoglobins, whereas peroxidase activity requires a ferric resting state. The enzymatic activity of DHP is most similar to that of cytochrome *c* peroxidase. Hydrogen peroxide (H_2O_2) binds to ferric heme iron to yield Compound II and a protein radical according to the reaction $AA + P{-}Fe^{III}{-}H_2O_2 \rightarrow AA^{+\cdot} + P{-}Fe^{IV}{=}O + H_2O$, where P is the protoporphyrin IX moiety of the heme and AA is an amino acid. The combination of Compound II and the radical cation $AA^{+\cdot}$ can act as a two-electron oxidant for phenolic substrates, as shown in mechanistic studies (Franzen *et al.*, 2007). We have shown elsewhere that the relevant form of the substrate is the phenolate form at physiological pH (Franzen *et al.*, 2007). However, the nature of substrate binding is complex and there is evidence for both internal and external binding interactions. When crystals of native DHP were soaked in a solution containing 4-iodophenol, the X-ray structure (PDB code

© 2009 International Union of Crystallography
Printed in Singapore – all rights reserved

1ewa) revealed that the phenol binds in an internal binding pocket (LaCount *et al.*, 2000). However, both kinetic analyses and NMR data indicated that the substrate-binding site is on the exterior of DHP (Franzen *et al.*, 2007; Davis *et al.*, 2008). Although it is not presently understood how DHP switches between its hemoglobin (dioxygen-binding) and peroxidase (dioxygen-cleaving) functions, substrate localization in the distal pocket has not been previously observed in globins and may play a regulatory role (Belyea *et al.*, 2005).

It is important to understand the ligation of the heme iron in DHP in light of its bifunctional nature. The ferric iron in methemoglobin and metmyoglobin is six-coordinate (Katz *et al.*, 1994; Royer, 1994; Liu *et al.*, 2001;Vojtechovsky *et al.*, 1999; Yang & Phillips, 1996; Nardini *et al.*, 1995; Della Longa *et al.*, 2003). In contrast, the heme iron is usually five-coordinate in ferric heme peroxidases (Hashimoto *et al.*, 1986; Chouchane *et al.*, 2000; Cheek *et al.*, 1999; Yonetani & Anni, 1987; de Ropp *et al.*, 1991; Andersson *et al.*, 1987; Kuila *et al.*, 1985; Yamazaki *et al.*, 1981; Wang *et al.*, 1990; Kunishima *et al.*, 1996), although it can be six-coordinate provided that the sixth heme iron ligand is sufficiently labile (Badyal *et al.*, 2006). The first published structure of native DHP, determined at room temperature, showed a water molecule in the distal pocket which was not located within bonding distance of the heme iron (PDB code 1ew6; LaCount *et al.*, 2000). In contrast, in structures determined at 100 K the ligands bound to the heme iron are stabilized by hydrogen bonding to the distal histidine His55 (Serrano *et al.*, 2007). A strong interaction of His55 with heme iron ligands is observed in the ferric metaquo form and oxy ferrous form of the C73S mutant. These structures have PDB codes 2qfk and 2qfn, respectively (Serrano *et al.*, 2007).

The hydrogen bonding of His55 to heme iron ligands, such as H_2O or O_2, may play a significant role in the peroxidase reactivity of DHP because it potentially regulates H_2O or O_2 displacement from the heme iron when the substrate interacts with the protein as required for peroxidase catalysis (Serrano *et al.*, 2007). The displacement of H_2O or O_2 from the heme iron is required for H_2O_2 binding, which is the first step of the catalytic cycle. However, the hypothesis that the distal histidine conformation is related to heme iron ligation must be reconciled with the observation of two conformations of His55 in the room-temperature X-ray crystal structure (LaCount *et al.*, 2000). The distal His55 residue was observed in both a closed conformation in the distal pocket and an open solvent-exposed conformation in the 1ew6 structure determined at room temperature. The correlation of these conformations with heme ligation is still not clear. In this report, we address the issue by determining the X-ray crystal structure of the deoxy form of DHP at 100 K.

The existence of multiple conformations of the distal histidine is a key structural feature that is common to both DHP and sperm whale myoglobin (SWMb; Tian *et al.*, 1993; Nienhaus *et al.*, 2006; Yang & Phillips, 1996). Although DHP is a dimeric hemoglobin, its subunits appear to act with relative independence. No cooperativity has so far been observed in any binding studies of substrate or heme iron ligand. Moreover, the intersubunit contacts consist of two salt bridges and are consequently relatively weak. In SWMb, a local conformational equilibrium between the open and closed distal pocket states can be triggered by pH variation (Morikis *et al.*, 1989; Tian *et al.*, 1993; Yang & Phillips, 1996). When the pH is lowered, the distal histidine HisE7 becomes protonated and rotates about the $C^{\alpha}-C^{\beta}$ bond towards the solvent (Morikis *et al.*, 1989; Tian *et al.*, 1993; Yang & Phillips, 1996). In the native DHP structure, His55 is displaced from the distal pocket when the a substrate analog 4-iodophenol binds in the internal binding site (LaCount *et al.*, 2000). In the metaquo structure of the recombinant wild-type DHP, the distal His55 is only observed in the closed conformation (Serrano *et al.*, 2007; Saga *et al.*, 1991; Tian *et al.*, 1993). Based on these observations, it appears that His55 is stabilized by hydrogen bonding to heme ligands and is observed in the open conformation when the heme is five-coordinate (*i.e.* when no ligand is present to act as a hydrogen-bond partner with His55) or on binding of 4-iodophenol in the distal pocket. The room-temperature DHP X-ray crystal structure shows that the distal histidine has significant conformational flexibility compared with ferric (metaquo) SWMb at pH $\simeq$ 6 (Kachalova *et al.*, 1999). Since the open conformation of SWMb is observed at pH 4 but not at pH 6 (at 277 K; Yang & Phillips, 1996), there is clearly a difference in the pK_a of the histidine of DHP relative to SWMb that requires explanation.

A number of heme proteins undergo conformational rearrangements, which can be triggered by a change in pH, in the oxidation state of the iron (Williams *et al.*, 1997; Badyal *et al.*, 2006) or by substrate binding. For example, a ligand switch in the refolding of mitochondrial cytochrome *c* involves a displacement of His by Met in a His–His coordinated heme *c* in the last stage of the folding process near neutral pH (Elove *et al.*, 1994; Colon *et al.*, 1996; Takahashi *et al.*, 1997; Yeh *et al.*, 1997). A similar change of ligation takes place in cytochrome cd_1 at the *c* heme during catalysis of the conversion of nitrite to nitric oxide (Williams *et al.*, 1997). An intrinsic mobility of the distal histidine was observed in the structure of the W41A mutant of ascorbic peroxidase. In the mutant, the distal histidine His42 binds to ferric heme iron (Badyal *et al.*, 2006). Binding of the substrate triggers a conformational change in which His42 dissociates from the heme. A similar conformational rearrangement occurs upon reduction of the heme iron, so that His42 dissociates from the iron in the ferrous form of W41A (Badyal *et al.*, 2008). The structure of deoxy DHP presented here shows that His55 is quite flexible when the heme is five-coordinate. The flexibility of the distal histidine in the deoxy DHP structure presents a contrast with the six-coordinate form where His55 is clearly in the distal pocket and is strongly associated with the sixth ligand, whether it is H_2O or O_2.

2. Material and methods

2.1. Protein purification, characterization and crystallization

Recombinant wild-type DHP was prepared and purified in the ferric form as described previously (Serrano *et al.*, 2007).

Table 1
Data-collection and refinement statistics for deoxy ferrous wild-type DHP.

Values in parentheses are for the highest resolution shell.

Data collection	
Wavelength (Å)	1.0000
Space group	$P2_12_12_1$
Unit-cell parameters (Å)	a = 57.5, b = 67.2, c = 69.1
Resolution (Å)	35.00–1.26 (1.29–1.26)
Unique reflections	68067 (4982)
Completeness (%)	98.43 (98.27)
$R_{\rm merge}$† (%)	0.057 (0.411)
$I/\sigma(I)$	18.3 (2.1)
Redundancy	3.5 (3.2)
Refinement	
$R_{\rm work}$‡ (%)	17.6 (24.7)
$R_{\rm free}$§ (%)	19.7 (28.1)
No. of protein atoms	2768
No. of solvent atoms	296
R.m.s.d. from ideal geometry	
Bond lengths (Å)	0.007
Bond angles (°)	1.208
Ramachandran plot¶ (%)	
Most favored region	94.8
Additional allowed region	5.2

† $R_{\rm merge} = \sum_{hkl}\sum_i |I_i(hkl) - \langle I(hkl)\rangle|/\sum_{hkl}\sum_i I_i(hkl)$, where $I_i(hkl)$ is the ith measurement and $\langle I(hkl)\rangle$ is the weighted mean of all measurements of $I(hkl)$. ‡ $R_{\rm work} = \sum |F_{\rm o} - F_{\rm c}|/\sum |F_{\rm o}|$, where $F_{\rm o}$ are observed and $F_{\rm c}$ are calculated structure factors. § $R_{\rm free}$ is the R factor for a subset (5%) of reflections selected previously and not included in refinement. ¶ Calculated using *PROCHECK* (Laskowski *et al.*, 1993).

The integrity of the protein was analyzed by assessing its enzymatic activity toward 2,4,6-tribromophenol (TBP), a natural substrate of DHP (Belyea *et al.*, 2005; Franzen *et al.*, 2006). Crystals were grown by the hanging-drop vapor-diffusion method from 0.2 *M* ammonium sulfate and 26–34% polyethylene glycol 4000 at 277 K. The starting protein concentration was 8 mg ml^{-1}. The pH of the drop solution was 5.9. Diffraction-quality crystals were obtained within one week and ranged in size from 0.2 to 0.7 mm in the largest dimension. The crystals grown in the ferric form were reduced in 20 m*M* sodium dithionite solution/mother liquor for 20 min under anaerobic conditions. For X-ray data collection at low temperatures, the crystals were removed from the reducing solution and cryoprotected by brief immersion in 10 µl 0.2 *M* ammonium sulfate solution containing 32% polyethylene glycol 4000 and 15% polyethylene glycol 400, mounted in a nylon loop and rapidly cryocooled in liquid nitrogen. The crystals belonged to space group $P2_12_12_1$, with unit-cell parameters a = 57.5, b = 67.2, c = 69.1 Å. The solvent content of the crystal was about 50% and the asymmetric unit contained two subunits.

2.2. X-ray data collection and structure refinement

X-ray diffraction data for deoxy wild-type DHP were collected at 100 K using a MAR 225 detector at the Advanced Photon Source (Argonne, Illinois, USA) using an X-ray wavelength of λ = 1.0 Å. The crystals diffracted to 1.22 Å resolution. The data were processed using the *HKL*-2000 program suite (Otwinowski & Minor, 1997). The structure was solved by molecular replacement with the program *Phaser* (McCoy *et al.*, 2005) at 3 Å resolution, using as a search model two polypeptide chains and two heme molecules from the asymmetric unit of the native DHP structure (PDB code 1ew6; LaCount *et al.*, 2000). In order to eliminate model bias, OMIT maps were constructed with *CNS* (Brünger *et al.*, 1998).

Table 2
Comparison of heme iron and distal and proximal histidine parameters.

The values are tabulated for subunit *A* of the asymmetric unit. Heme restraints are derived from the monomer library of the *REFMAC*5 program from the *CCP*4 suite (Collaborative Computational Project, Number 4, 1994), with no restraints on Fe axial-ligand bond lengths.

	Protein form		
	Deoxy ferrous wild type	Metaquo wild type† (2qfk)	Oxy ferrous C73S† (2qfn)
Fe—His89 $N^{\varepsilon 2}$ (Å)	2.18	2.09	2.15
Fe—His55 $N^{\varepsilon 2}$‡ (Å)	—	4.75	5.13
Fe to porphyrin plane (Å)	0.25	0.04	0.09

† Compiled from the published structures of DHP at 100 K (PDB codes 2qfk and 2qfn). ‡ Distance to the His55 conformer located inside the distal cavity.

Approximately 20 residues in each chain in the deoxy wild-type DHP could be modeled in alternative conformations and their occupancies were adjusted until there was no significant $F_{\rm o} - F_{\rm c}$ density. Using $F_{\rm o} - F_{\rm c}$ electron density contoured at 3σ, 290 water molecules were positioned into the structure using *Coot* (Emsley & Cowtan, 2004). The final model was obtained by iterative positional and isotopic *B*-factor refinement using *REFMAC*5 (Murshudov *et al.*, 1997) from the *CCP*4 suite of programs (Collaborative Computational Project, Number 4, 1994). Simulated-annealing and composite OMIT maps were constructed using *CNS*. The final model of the deoxy wild-type DHP structure contained two protein molecules in the asymmetric unit, three sulfate ions and 290 water molecules. Relevant X-ray data-collection and refinement statistics are summarized in Table 1.

3. Results and discussion

Crystals of recombinant wild-type DHP were produced as previously described (Serrano *et al.*, 2007) using protein in the ferric (Fe^{III}) oxidation state as determined by UV–Vis spectroscopy (Soret maximum at 406 nm). Preparation of crystals of the deoxy ferrous form of wild-type DHP was attempted using two different methods. In the first method, DHP was reduced using sodium dithionite and set up for crystallization in an anaerobic atmosphere. However, no diffraction-quality crystals grew under these conditions. In the second method, crystals of DHP were reduced by soaking in sodium dithionite dissolved in the mother liquor. The second method produced diffraction-quality crystals. A diffraction data set was collected at 100 K on the SER-CAT 22-BM beamline at the Advanced Photon Source (Argonne, Illinois, USA) and the structure was refined to a resolution of 1.22 Å with an R factor of 18.5% (Table 1). The deoxy wild-type DHP crystallized with two molecules in the asymmetric unit, as observed in the original structural analysis of DHP (Zhang *et al.*, 1996).

3.1. Heme iron ligation in the structure

The proximal histidine His89 is the fifth coordination ligand of the heme iron in DHP. The Fe—N^{ε} bond length refines to 2.18 Å. The heme Fe atom is displaced 0.25 Å below the porphyrin plane on the proximal side (Table 2). The doming of the heme iron can be seen in the $2F_o - F_c$ electron-density map shown in Fig. 1. In the metaquo ferric and oxy ferrous DHP structures, the six-coordinate Fe atom is positioned at a distance of 0.04 and 0.09 Å below the porphyrin plane, respectively (Serrano *et al.*, 2007). The iron displacement in the deoxy form is similar to observations in SWMb (Cameron *et al.*, 1993) and is attributable to the change in spin state and coordination geometry. The heme iron in DHP behaves like SWMb in that it moves out of the heme plane in response to dissociation of a ligand from the six-coordinate low-spin heme to form a five-coordinate high-spin heme (Schlichting *et al.*, 1994; Hartmann *et al.*, 1996; Chu *et al.*, 2000). The core-size expansion drives the iron out of the heme plane and serves as a trigger for the protein-structure change that gives rise to the cooperative oxygen binding observed in the human hemoglobin tetramer (Hoffman *et al.*, 1972; Perutz, 1970; Brucker *et al.*, 1996; Franzen *et al.*, 1994).

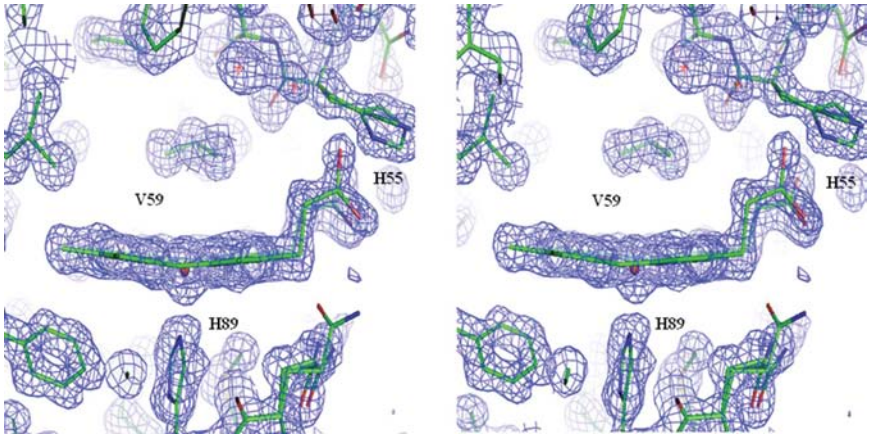

Figure 1
Stereo drawing of the $2F_o - F_c$ electron-density map for deoxy ferrous DHP. The map was contoured at 1.3σ and the coordinates shown correspond to chain *A*.

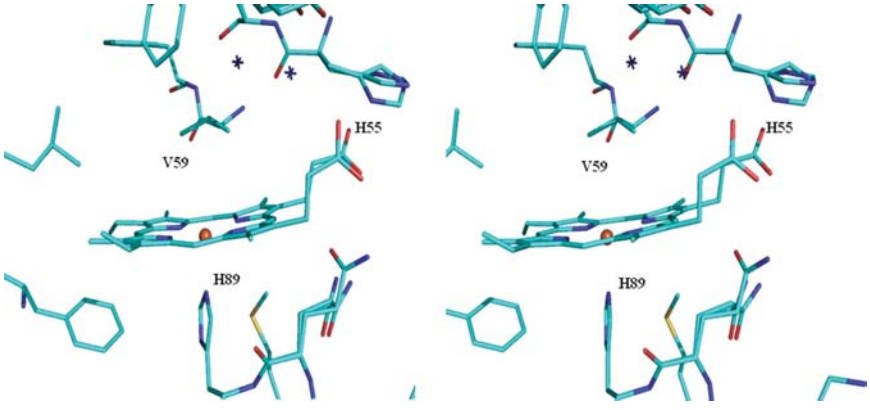

Figure 2
Stereoview of the distal-pocket region of deoxy ferrous DHP.

3.2. Distal histidine conformations in DHP

His55 is observed in two conformations in the structure of deoxy wild-type DHP, both of which correspond to the solvent-exposed or open position (Fig. 2). Based on OMIT maps, it was possible to place the distal histidine in a third conformation in the distal pocket (not shown) with an occupancy of 44% (46% in chain *B*). However, this structure was deemed to be inappropriate based on the lack of electron density in four atom positions on the side of the imidazole ring closest to the heme. The alternative model with water instead of His55 in the distal pocket resulted in a poorer fit to the electron-density map. Since His55 ring electron density is missing for the lower portion of the ring in the best-fit model, we concluded that the density corresponds to a water atom. Fig. 1 shows that the two His55 conformations in the solvent-exposed open conformation are clearly well represented by the electron density, but there is not sufficient electron density in the internal or closed position to justify placement of His55. The difficulty in fitting the region of the density in the distal pocket is likely to arise from ring torsional dynamics of the histidine that are responsible for the lack of observable density in this portion of the structure.

There are two well defined conformations of His55 that are located in a solvent-exposed site that is more than 9.5 Å away from the heme plane. The two solvent-exposed conformations of His55 are not completely separated and their occupancies are 70 and 30%, respectively (87 and 13% in chain *B*). The C^{α}, C^{β} and C^{γ} atoms of those two conformations overlap, but the imidazole planes have different rotation angles around the C^{β}—C^{γ} bond. The N^{δ} atom in the conformation with 70% occupancy (chain *A*) is positioned at a hydrogen-bonding distance (2.85 Å) from heme propionate 6.

The deoxy ferrous DHP structure differs from those of metaquo ferric DHP and oxy ferrous DHP, as shown in Figs. 3 and 4, respectively (Serrano *et al.*, 2007). There is no water or other ligand in the vicinity of the heme iron in the deoxy structure. The solvent-exposed conformations of the distal histidine in the deoxy structure can be contrasted with the internal conformation of the distal histidine in the metaquo DHP (2qfk) and oxy ferrous C73S (2qfn) structures (Serrano *et al.*, 2007). These differences are of great interest because of the key role played by the distal histidine in both globin oxygen binding and in peroxidase catalysis.

Although the enzymatic activity of DHP is similar to that of heme peroxidases, it has the structural characteristics of the globin

protein family. The conformation of the distal histidine in the six-coordinate metaquo adduct of DHP is consistent with the structures of ferric myoglobins and hemoglobins (Serrano *et al.*, 2007). Likewise, the distal histidine of DHP in the oxy ferrous form is analogous to the structure of oxy ferrous SWMb (Phillips, 1980; Brucker *et al.*, 1996). However, the conformation of the distal histidine in the deoxy DHP structure is unique in terms of its conformational flexibility.

In the deoxy SWMb structure (Cameron *et al.*, 1993), there is a noncoordinated water molecule in the distal pocket that is in a position to form strong hydrogen bonds to N^{ε} of the distal histidine. In SWMb, the distal-pocket water of the deoxy form is eliminated in the H64L mutant (Christian *et al.*, 1997). Elsewhere, we have shown the similarity of the H64V heme environment to DHP in the context of NO recombination kinetics (Franzen *et al.*, 2006). Replacement of the histidine with an aliphatic amino acid makes the distal pocket more hydrophobic in both H64L and H64V SWMb. Comparison with the SWMb mutants leads to the conclusion that the hydrophobic nature of the distal pocket in DHP (Serrano *et al.*, 2007) may contribute to the absence of a water molecule in this pocket in the deoxy structure.

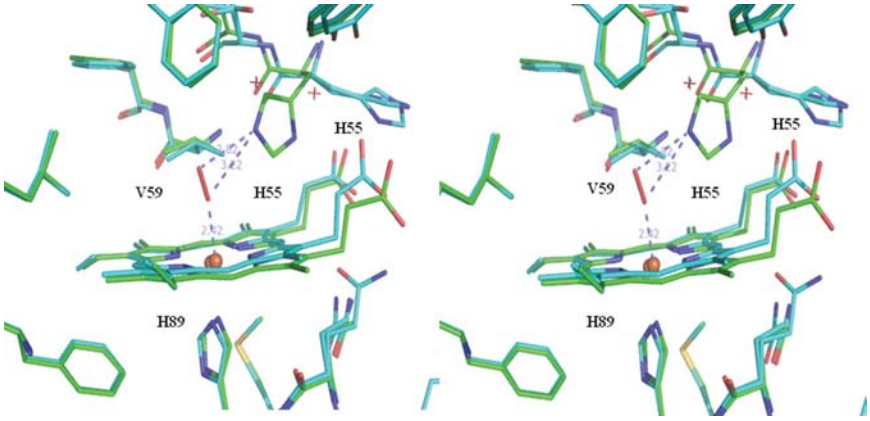

Figure 3
Stereoview of an overlay of the distal-pocket region of deoxy ferrous DHP (colored blue) and oxy ferrous DHP (PDB code 2qfn, colored green).

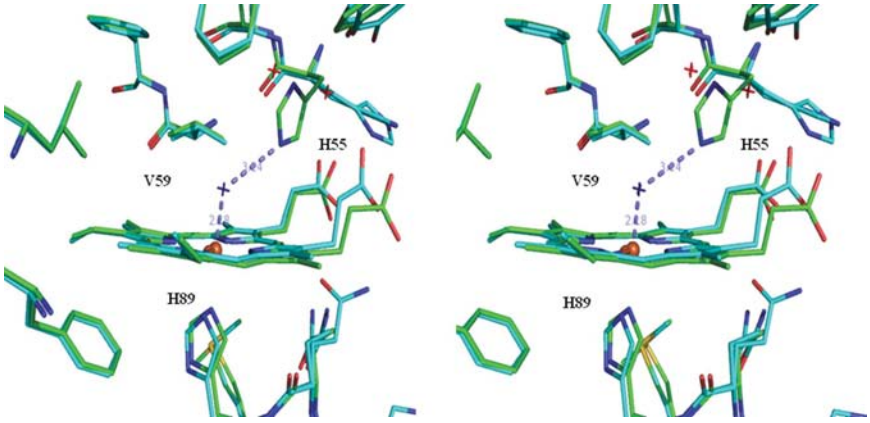

Figure 4
Stereoview of an overlay of the distal-pocket region of deoxy ferrous DHP (colored cyan) and metaquo ferric DHP (PDB code 2qfn, colored green).

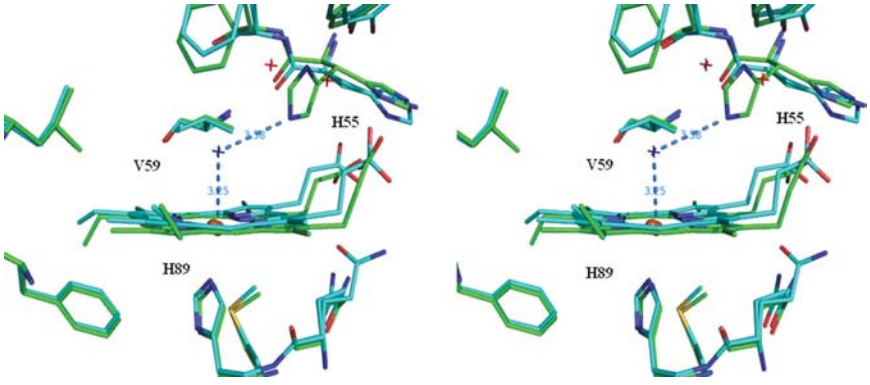

Figure 5
Stereoview of an overlay of the distal-pocket region of deoxy ferrous DHP (colored cyan) and the ferric form of native DHP at room temperature (PDB code 1ew6, colored green).

Based on the deoxy structure, we can begin to understand the origin of the two conformations of His55 in the room-temperature X-ray structure of ferric DHP (LaCount *et al.*, 2000). An overlay of the 100 K deoxy DHP structure with the room-temperature ferric DHP structure (1ew6) in Fig. 5 shows subtle differences in the open His55 conformations. The most obvious difference is that there is essentially no well defined conformation for His55 in the internal or closed conformation. There appear to be even greater dynamics of His55 in the deoxy structure than in the room-temperature ferric DHP structure. Based on previous work, we hypothesized that the ligation state of the water in the ferric form of DHP depends on temperature (Serrano *et al.*, 2007). Fig. 4 shows a water molecule bound to the heme iron in ferric (metaquo) DHP that forms a strong hydrogen bond to His55. As a consequence, His55 is observed only in the closed conformation in the metaquo DHP structure at 100 K (Serrano *et al.*, 2007). We hypothesize that at ambient temperature the ferric heme iron adduct consists of an equilibrium between five-coordinate and six-coordinate metaquo forms. If the His55 conformation is coupled to the heme iron ligand by hydrogen bonding, then both open and closed conformations would be expected in the room-temperature structure corresponding to the five- and six-coordinate adducts, respectively.

The hypothesis of stabilization by the heme iron ligand must also take into

account the protonation state of the distal histidine. The solvent-exposed conformation of the distal histidine is analogous to the open conformation of His64 in SWMb that was observed in a low-pH (pH 4.0) environment (Sage *et al.*, 1991; Tian *et al.*, 1996). The solvent-exposed or open conformation observed by X-ray crystallography is likely to be associated with the protonation of His64 in SWMb (Yang & Phillips, 1996). At low pH the oxygen-dissociation rate increases dramatically, suggesting that the hydrogen bond between the distal histidine and the bound O_2 is important for the stabilization of bound oxygen in the closed conformation and is disrupted in the open conformation. According to this hypothesis, the open form of deoxy ferrous DHP would also provide an open channel that allows ligand diffusion between the solution and the heme. According to this hypothesis, the distal histidine stabilizes the oxygen on the heme iron by hydrogen-bond formation, which is consistent with the X-ray structure (Serrano *et al.*, 2007)

The difference between room-temperature and 100 K crystal structures may depend on the temperature-dependence of the pK_a of the distal histidine (Braunstein *et al.*, 1993; Nienhaus *et al.*, 2008). The distal histidine of SWMb, His64, has a pK_a of ∼4.5 at room temperature, which implies that His64 will be in the closed conformation at pH 6, which was used for crystallization. FTIR spectroscopy of SWMb indicates that the fraction of the open conformation increases as the temperature is lowered (Braunstein *et al.*, 1993; Nienhaus *et al.*, 2008). In DHP there is the additional factor that binding of a substrate analog in the internal binding site can force the distal histidine into the open or solvent-exposed conformation (LaCount *et al.*, 2000), but this effect may also be coupled with protonation of the distal histidine. Since molecular binding in the internal site also displaces His55 (Smirnova *et al.*, 2008), conformational flexibility may also be associated with the lack of a hydrogen-bond partner in the substrate-bound form. Thus, the conformation of the distal histidine of DHP has been shown to be determined by interrelated interactions between the protonation state, the heme iron ligand and the presence of substrate.

4. Conclusion

The X-ray crystal structure of deoxy DHP strongly resembles the X-ray crystal structures of deoxy SWMb in the geometry of the heme iron, but shows a greater conformational flexibility of the distal histidine His55. The heme iron is significantly displaced out of the porphyrin plane compared with six-coordinate ferric adducts and this heme doming is comparable to that of deoxy SWMb (Vojtechovsky *et al.*, 1999; Kachalova *et al.*, 1999). The comparison with myoglobin is relevant since the intersubunit interactions of the DHP dimer are relatively weak. Most X-ray crystal structures of SWMb have been obtained at pH 6, which is also the pH that is optimal for crystallization of DHP. The observation of His55 in the open conformation at pH 6 may be a consequence of the temperature-dependence of the pK_a of the distal histidine (Braunstein *et al.*, 1993; Nienhaus *et al.*, 2008). As the temperature is lowered, the pK_a of the distal histidine increases and the greater population of the protonated imidazolium ring leads to a larger population of the solvent-exposed conformation. The only deoxy SWMb X-ray crystal structure at cryogenic temperature was obtained at pH 7, which was necessary to ensure that the distal histidine remained in the closed conformation (Vojtechovsky *et al.*, 1999). The systematic study of histidine conformation in SWMb as a function of pH conducted by Yang & Phillips (1996) at 277 K shows a difference from DHP. While SWMb requires a pH of ∼4.5 to show a significant fraction of distal histidine (His64) residues in the open conformation, the room-temperature DHP structure shows 50% of the His55 residues in the open conformation at pH 6 (LaCount *et al.*, 2000). These results suggest that the conformational rearrangements of His55 are intrinsically different in DHP. One possible difference is the fact that the heme is buried 1.5 Å more deeply in the globin relative to SWMb (Serrano *et al.*, 2007). The displacement of the heme deeper into the globin implies that the histidine is more distant from the heme iron in DHP and therefore more labile. On the other hand, the lability of the distal histidine is restricted by hydrogen-bonding interactions with ligands bound to the heme iron, which are strong in the metaquo DHP and oxy ferrous C73S structures at 100 K (Serrano *et al.*, 2007). Thus, it is suggested that a combination of the ligation state of the iron and the protonation state of the histidine determine the His55 conformation.

The structure presented here represents an important aspect of coupling of a protein motion with heme ligation that is likely to be associated with both the hemoglobin and peroxidase functions of DHP. The flexibility of His55 accounts for the high escape rate for carbon monoxide (CO) in photolyzed DHP–CO and therefore with the ease of ligand exchange at the heme iron that is required for activation by H_2O_2 (Nienhaus *et al.*, 2006). The coupled motion of His55 with the substrate analog 4-iodophenol, which binds in an unusual internal binding site, must also depend on the flexibility of the distal histidine (LaCount *et al.*, 2000). Since the binding of substrate analogs in the internal pocket also displaces bound water in the metaquo form (Smirnova *et al.*, 2008), the displacement of His55 to the open form observed in the deoxy DHP structure is driven both by steric interactions and by loss of stabilization owing to hydrogen bonding. These features are likely to regulate the activity of the two functions of DHP.

We acknowledge financial support for this work from Army Research Office Grant 52278-LS. We thank Dr Zhongmin Jin at SER-CAT (Advanced Photon Source) for synchrotron data collection. The Advanced Photon Source is supported by the US Department of Energy, Office of Science, Office of Basic Energy Sciences under Contract No. W-31-109-End-38. We thank Dr Robert Rose, Department of Molecular and Structural Biochemistry at NCSU for insightful discussions.

References

Andersson, L. A., Renganathan, V., Loehr, T. M. & Gold, M. H. (1987). *Biochemistry*, **26**, 2258–2263.

Badyal, S. K., Joyce, M. G., Sharp, K. H., Seward, H. E., Mewies, M., Basran, J., Macdonald, I. K., Moody, P. C. E. & Raven, E. L. (2006). *J. Biol. Chem.* **281**, 24512–24520.

Belyea, J., Belyea, C. M., Lappi, S. & Franzen, S. (2006). *Biochemistry*, **45**, 14275–14284.

Belyea, J., Gilvey, L. B., Davis, M. F., Godek, M., Sit, T. L., Lommel, S. A. & Franzen, S. (2005). *Biochemistry*, **44**, 15637–15644.

Braunstein, D. P., Chu, K., Egeberg, K. D., Frauenfelder, H., Mourant, J. R., Nienhaus, G. U., Ormos, P., Sligar, S. G., Springer, B. A. & Young, R. D. (1993). *Biophys. J.* **65**, 2447–2454.

Brucker, E. A., Olson, J. S. & Phillips, G. N. Jr (1996). *J. Biol. Chem.* **271**, 25419–25422.

Brünger, A. T., Adams, P. D., Clore, G. M., DeLano, W. L., Gros, P., Grosse-Kunstleve, R. W., Jiang, J.-S., Kuszewski, J., Nilges, M., Pannu, N. S., Read, R. J., Rice, L. M., Simonson, T. & Warren, G. L. (1998). *Acta Cryst.* D**54**, 905–921.

Cameron, A. D., Smerdon, S. J., Wilkinson, A. J., Habash, J., Helliwell, J. R., Li, T. & Olson, J. S. (1993). *Biochemistry*, **32**, 13061–13070.

Cheek, J., Mandelman, D., Poulos, T. L. & Dawson, J. (1999). *J. Biol. Inorg. Chem.* **4**, 64–72.

Chouchane, S., Lippai, I. & Magliozzo, R. S. (2000). *Biochemistry*, **39**, 9975–9983.

Christian, J. F., Unno, M., Sage, J. T., Champion, P. M., Chien, E. & Sligar, S. G. (1997). *Biochemistry*, **36**, 11198–11204.

Chu, K., Vojtchovsky, J., McMahor, B., Sweet, R., Berendzen, J. & Schlichting, I. (2000). *Nature (London)*, **403**, 921–923.

Collaborative Computational Project, Number 4 (1994). *Acta Cryst.* D**50**, 760–763.

Colon, W., Elove, G. A., Wakem, L. P., Sherman, F. & Roder, H. (1996). *Biochemistry*, **35**, 5538–5549.

Davis, M. F., Gracz, H., Vendeix, F. A. P., Gilvey, L. B., Somasundaram, A., Decatur, S. M. & Franzen, S. (2008). In the press.

Della Longa, S., Arcovito, A., Benefatto, M., Congiu-Castellano, A., Girasole, M., Hazemann, J. L. & Lo Bosco, A. (2003). *Biophys. J.* **85**, 549–558.

Elove, G. A., Bhuyan, A. K. & Roder, H. (1994). *Biochemistry*, **33**, 6925–6935.

Emsley, P. & Cowtan, K. (2004). *Acta Cryst.* D**60**, 2126–2132.

Franzen, S., Gilvey, L. B. & Belyea, J. (2007). *Biochim. Biophys. Acta*, **1774**, 121–130.

Franzen, S., Jasaitis, A., Belyea, J., Brewer, S. H., Casey, R., MacFarlane, A. W. IV, Stanley, R., Vos, M. H. & Martin, J.-L. (2006). *J. Phys. Chem. B*, **110**, 14483–14493.

Franzen, S., Lambry, J.-C., Bohn, B., Poyart, C. & Martin, J.-L. (1994). *Nature Struct. Biol.* **1**, 230–233.

Hartmann, H., Zinser, S., Komninos, P., Schneider, R. T., Nienhaus, G. U. & Parak, F. (1996). *Proc. Natl. Acad. Sci. USA*, **93**, 7013–7016.

Hashimoto, S., Teraoka, J., Inubushi, T., Yonetani, T. & Kitagawa, T. (1986). *J. Biol. Chem.* **261**, 11110–11118.

Hoffman, B. M., Spilburg, C. A. & Petering, D. H. (1972). *Cold Spring Harbor Symp. Quant. Biol.* **36**, 343–348.

Kachalova, G. S., Popov, A. N. & Bartunik, H. D. (1999). *Science*, **284**, 473–476.

Katz, D. S., White, S. P., Huang, W., Kumar, R. & Christianson, D. W. (1994). *J. Mol. Biol.* **244**, 541–553.

Kuila, D., Tien, M., Fee, J. A. & Ondrias, M. R. (1985). *Biochemistry*, **24**, 3394–3397.

Kunishima, N., Amada, F., Fukujama, K., Kawamoto, M., Maesunaga, T. & Matsubara, H. (1996). *FEBS Lett.* **378**, 291–294.

LaCount, M. W., Zhang, E., Chen, Y. P., Han, K., Whitton, M. M., Loncoln, D. E., Woodin, S. A. & Lebioda, L. (2000). *J. Biol. Chem.* **275**, 18712–18716.

Laskowski, R. A., MacArthur, M. W., Moss, D. S. & Thornton, J. M. (1993). *J. Appl. Cryst.* **26**, 283–291.

Liu, X.-Z., Li, S.-L., Jing, H., Liang, Y.-H., Hua, Z.-Q. & Lu, G.-Y. (2001). *Acta Cryst.* D**57**, 775–783.

McCoy, A. J., Grosse-Kunstleve, R. W., Storoni, L. C. & Read, R. J. (2005). *Acta Cryst.* D**61**, 458–464.

Morikis, D., Champion, P. M., Springer, B. A. & Sligar, S. G. (1989). *Biochemistry*, **28**, 4791–4800.

Murshudov, G. N., Vagin, A. A. & Dodson, E. J. (1997). *Acta Cryst.* D**53**, 240–255.

Nardini, M., Tarricone, C., Rizzi, M., Lania, A., Desideri, A., De Danctie, G., Coletta, M., Petruzzeli, R., Ascenzi, P., Coda, A. & Bolognesi, M. (1995). *J. Mol. Biol.* **247**, 459–465.

Nienhaus, K., Deng, P., Belyea, J., Franzen, S. & Nienhaus, G. U. (2006). *J. Phys. Chem. B*, **110**, 13264–13276.

Nienhaus, K., Palladino, P. & Nienhaus, G. U. (2008). *Biochemistry*, **47**, 935–948.

Otwinowski, Z. & Minor, W. (1997). *Methods Enzymol.* **276**, 307–326.

Perutz, M. F. (1970). *Nature (London)*, **228**, 726–734.

Phillips, S. E. V. (1980). *J. Mol. Biol.* **142**, 531–554.

Ropp, J. S. de, La Mar, G. N., Wariishi, H. & Gold, M. H. (1991). *J. Biol. Chem.* **266**, 15001–15008.

Royer, W. E. Jr (1994). *J. Mol. Biol.* **235**, 657–681.

Sage, J. T., Morikis, D. & Champion, P. M. (1991). *Biochemistry*, **30**, 1227–1237.

Schlichting, I., Berendzen, J., Phillips, G. & Sweet, R. (1994). *Nature (London)*, **137**, 808–812.

Serrano, V. de, Chen, Z., Davis, M. F. & Franzen, S. (2007). *Acta Cryst.* D**63**, 1094–1101.

Smirnova, T. I., Weber, R. T., Davis, M. F. & Franzen, S. (2008). *J. Am. Chem. Soc.* **130**, 2128–2129.

Takahashi, S., Yeh, S.-R., Das, T. K., Chan, C.-K., Gottfried, D. S. & Rousseau, D. L. (1997). *Nature Struct. Biol.* **4**, 44–50.

Tian, W., Saga, J. & Champion, P. (1993). *J. Mol. Biol.* **233**, 155–156.

Tian, W., Saga, J., Champion, P., Chien, E. & Sligar, S. (1996). *Biochemistry*, **35**, 3487–3502.

Vojtechovsky, J., Chu, K., Berendzen, J., Sweet, R. M. & Schlichting, I. (1999). *Biophys. J.* **77**, 2153–2174.

Wang, J., Mauro, M., Edwards, S. L., Oatley, S. J., Fishel, L. A., Ashford, V. A., Xuong, N.-H. & Kraut, J. (1990). *Biochemistry*, **29**, 7160–7173.

Williams, P. A., Fülöp, V., Garman, E. F., Saunders, N. F. W., Ferguson, S. J. & Hajdu, J. (1997). *Nature (London)*, **389**, 406–412.

Yamazaki, I., Tamura, M. & Nakajima, R. (1981). *Mol. Cell. Biochem.* **40**, 143–153.

Yang, F. & Phillips, G. N. (1996). *J. Mol. Biol.* **256**, 762–774.

Yeh, S.-R., Takahashi, S., Fan, B. & Rousseau, D. L. (1997). *Nature Struct. Biol.* **4**, 51–56.

Yonetani, T. & Anni, H. (1987). *J. Biol. Chem.* **262**, 9547–9554.

Zhang, E., Chen, Y. P., Roach, M. P., Lincoln, D. E., Lovell, C. R., Woodin, S. A., Dawson, J. H. & Lebioda, L. (1996). *Acta Cryst.* D**52**, 1191–1193.